AD-A095 460 NAVAL OCEAN SYSTEMS CENTER SAN DIEGO CA F/G 12/1
STATISTICS FOR PEAK VALUES OF MULTIPLE COHERENCE.(U)
SEP 80 D M KLAMER
UNCLASSIFIED NOSC/TR-628 NL

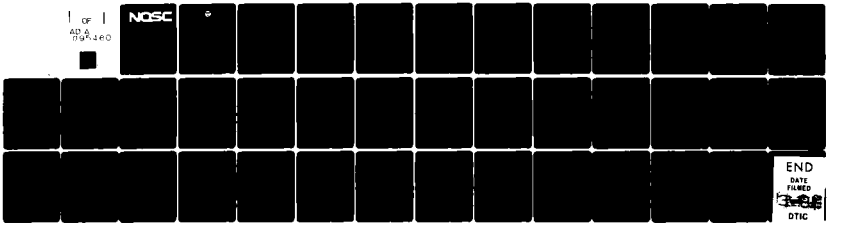

NOSC

NOSC TR 628

NOSC TR 628

Technical Report 628

STATISTICS FOR PEAK VALUES OF MULTIPLE COHERENCE

D.M. Klamer

28 September 1980

Final Report: October 1979 - September 1980

Prepared for
Naval Electronic Systems Command

Approved for public release; distribution unlimited

NAVAL OCEAN SYSTEMS CENTER
SAN DIEGO, CALIFORNIA 92152

NAVAL OCEAN SYSTEMS CENTER, SAN DIEGO, CA 92152

AN ACTIVITY OF THE NAVAL MATERIAL COMMAND

SL GUILLE, CAPT, USN
Commander

HL BLOOD
Technical Director

ADMINISTRATIVE INFORMATION

This work was performed from 1 October 1979 to 30 September 1980, under the sponsorship of NAVELEX 320. Funds were provided through Program Element 62711N, subproject XF11-101-100.

Released by
R. R. Smith, Head
Signal Processing and
Display Division

Under authority of
H. A. Schenck, Head
Undersea Surveillance
Department

ACKNOWLEDGEMENTS

The author is indebted to A. Smotkin, Code 7134, Signal Processing and Display Division, for programming assistance with the ROC curves associated with coherence, and to G. Miller, New Professional on tour in Code 713, for programming the multiple coherence results.

UNCLASSIFIED

SECURITY CLASSIFICATION OF THIS PAGE (When Data Entered)

(14) NOSC/TR-628

REPORT DOCUMENTATION PAGE

READ INSTRUCTIONS BEFORE COMPLETING FORM

1. REPORT NUMBER: NOSC Technical Report 628 (TR 628)	2. GOVT ACCESSION NO. AD-A095460 (9)
3. RECIPIENT'S CATALOG NUMBER	
4. TITLE (and Subtitle): STATISTICS FOR PEAK VALUES OF MULTIPLE COHERENCE.	5. TYPE OF REPORT & PERIOD COVERED: Final Report 1 October 1979 - September 1980
6. PERFORMING ORG. REPORT NUMBER	
7. AUTHOR(s): D. M. Klamer (10) (16) F11101	8. CONTRACT OR GRANT NUMBER(s) (17)
9. PERFORMING ORGANIZATION NAME AND ADDRESS: Naval Ocean Systems Center, San Diego, CA 92152	10. PROGRAM ELEMENT, PROJECT, TASK AREA & WORK UNIT NUMBERS: 62711N; XF11 101 100
11. CONTROLLING OFFICE NAME AND ADDRESS: Naval Electronic Systems Command, Washington, D.C. 20360	12. REPORT DATE: 28 September 1980
	13. NUMBER OF PAGES: 33
14. MONITORING AGENCY NAME & ADDRESS(if different from Controlling Office) (12) 34	15. SECURITY CLASS. (of this report): Unclassified
	15a. DECLASSIFICATION/DOWNGRADING SCHEDULE

16. DISTRIBUTION STATEMENT (of this Report)

Approved for public release; distribution unlimited.

17. DISTRIBUTION STATEMENT (of the abstract entered in Block 20, if different from Report)

18. SUPPLEMENTARY NOTES

19. KEY WORDS (Continue on reverse side if necessary and identify by block number)

multiple coherence
magnitude-squared coherence (MSC)
receiver operating characteristic (ROC) curves
Neyman-Pearson hypotheses test

20. ABSTRACT (Continue on reverse side if necessary and identify by block number)

The objective of this work is to determine the performance of the maximum (or peak) of estimates of the magnitude-squared coherence (MSC) on a passive ambiguity surface as a detection statistic.

The method chosen to measure the objective was the receiver operating characteristic (ROC) curves which plot the probability of detection versus the false alarm rate. To obtain the ROC curves, the probability distribution function of the maximum value of the MSC estimates for noise only, along with noise and signal present, are developed. These probability distribution and density functions are then used to establish a Neyman-Pearson hypotheses test for signal detection. The signal detection results are presented as ROC curves which depend on the size of the surface over which the maximum is taken, the true coherence, and the number of degrees of freedom of the individual estimates of the MSC. These results are then extended to multiple coherence.

DD FORM 1 JAN 73 1473 EDITION OF 1 NOV 65 IS OBSOLETE
S/N 0102-LF-014-6601

UNCLASSIFIED

SECURITY CLASSIFICATION OF THIS PAGE (When Data Entered)

34159

SUMMARY

OBJECTIVE

The objective of this work is to determine the performance of the maximum (or peak) of estimates of the magnitude-squared coherence (MSC) on a passive ambiguity surface as a detection statistic.

RESULTS

The method chosen to measure the objective was the receiver operating characteristic (ROC) curves which plot the probability of detection versus the false alarm rate. To obtain the ROC curves, the probability distribution function of the maximum value of the MSC estimates for noise only, along with noise and signal present, are developed. These probability distribution and density functions are then used to establish a Neyman-Pearson hypotheses test for signal detection. The signal detection results are presented as ROC curves which depend on the size of the surface over which the maximum is taken, the true coherence, and the number of degrees of freedom of the individual estimates of the MSC. These results are then extended to multiple coherence.

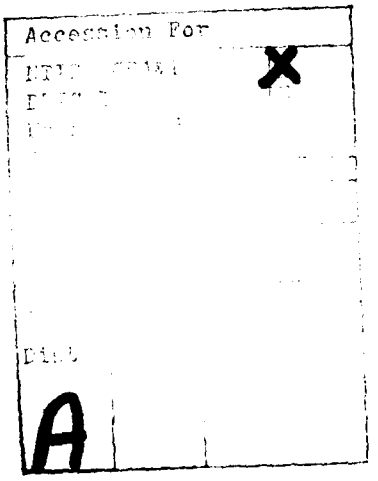

CONTENTS

1. INTRODUCTION

The determination of the probability distribution and density functions of the maximum (or peak) of estimates (of the magnitude-squared coherence) on a passive ambiguity surface is the main focus of this report. This peak value of the estimate of the magnitude-squared coherence (MSC) serves as a "data reduction" aid in processing the information contained in the passive ambiguity surface (PAS). We obtain the probability distribution and density functions in terms of the size of the surface over which the maximum is taken, the true coherence, and the number of degrees of freedom of each individual MSC estimate. These probability distribution and density functions are then used to characterize the signal detection performance of the maximum MSC estimate.

In Section 2 we present a review and necessary background on the MSC estimate for a single point on a PAS. The probability distribution function of the maximum value of the MSC estimates for noise only, along with noise and signal present, are developed in Section 3. These probability distribution and density functions are then used to establish a Neyman-Pearson type hypotheses test for signal detection in Section 4. The signal detection results are presented as ROC curves which depend on the size of the surface over which the maximum is taken, the true coherence, and the number of degrees of freedom of the individual estimates. In Section 5 we extend the results of Sections 3 and 4 to the case of the magnitude-squared multiple coherence. Section 6 concludes with some final remarks regarding the relationships between the parameters of the PAS and the detection performance.

2. BACKGROUND

Let $X_1(t)$ and $X_2(t)$ be real, zero-mean Gaussian random processes which are jointly wide-sense stationary. The correlation functions $R_{jk}(t)$ are defined by

$$R_{jk}(t) = E\left\{X_j(t+s)\, X_k(s)\right\}$$

for j, k = 1, 2, and the associated power spectral densities $\phi_{jk}(f)$ are assumed to exist with

$$\phi_{jk}(f) = \int_{-\infty}^{\infty} R_{jk}(t) \exp(-i\, 2\pi\, ft)\, dt,$$

for j, k = 1, 2. The magnitude-squared coherence (MSC) function is defined as the magnitude-squared of the cross-spectral density $\phi_{12}(f)$ divided by the product of the power spectral densities $\phi_{11}(f)\, \phi_{22}(f)$, i.e., the MSC function is defined by

$$\gamma^2(f) = \frac{|\phi_{12}(f)|^2}{\phi_{11}(f)\, \phi_{22}(f)} \qquad (1)$$

when $\phi_{jj}(f) > 0$, and by 0 otherwise. The MSC function $\gamma^2(f)$ measures the proportion of the power of X_1, at frequency f, attributable to the linear regression of X_1 on X_2 [1].

An estimate of $\gamma^2(f)$ is formed from N independent (i.e., no overlap) segments of data given by

$$\hat{\gamma}^2(f) = \frac{\left| \sum_{k=1}^{N} F_1(f;k)\, F_2^*(f;k) \right|^2}{\sum_{k=1}^{N} |F_1(f;k)|^2 \sum_{k=1}^{N} |F_2(f;k)|^2} \qquad (2)$$

where $F_i(f;k)$ is the Fourier coefficient at the frequency f from the k^{th} discrete Fourier transform (DFT) sample of the process $X_i(t)$. We note that $F_i(f;k)$ is a complex Gaussian random variable.

A passive ambiguity surface (PAS) is formed by compensating the MSC estimate for a range of time delays and doppler shifts. Specifically, to account for a time delay of τ and a doppler correction of θ radians, the estimate of the MSC becomes

$$\hat{\gamma}^2(f;\tau,\theta) = \frac{\left| \sum_{k=1}^{N} F_1(f;k)\, e^{-ik\theta}\, F_2^*(f;k-\tau) \right|^2}{\sum_{k=1}^{N} |F_1(f;k)|^2 \sum_{k=1}^{N} |F_2(f;k-\tau)|^2} \qquad (3)$$

The passive ambiguity surface consists of a "grid" of points over which the MSC estimate is computed for A_{td} distinct values of time delay $T = \{\tau_1, \ldots, \tau_{A_{td}}\}$ and for A_d distinct values of doppler $\Theta = \{\theta_1, \ldots, \theta_{A_d}\}$. Thus, the PAS contains a total of $A = A_{td} \cdot A_d$ points, each of which is an estimate of the MSC. Also, the spacing of the time delays and doppler shifts is assumed to give independent estimates of the magnitude-squared coherence. Again we note that $F_1(f;k)\, e^{-ik\theta}$ and $F_2^*(f;k-\tau)$ are both complex Gaussian random variables.

For the sake of completeness we review the distribution and density functions for the estimate of the MSC $\hat{\gamma}^2(\tau,\theta)$ at a single point of the PAS. The frequency f is assumed to be fixed, and thus, the dependency of $\hat{\gamma}^2(f;\tau,\theta)$ on f is suppressed. There are two cases to consider:

(a) Signal absent. In this case the true value of the MSC is assumed to be zero. The probability distribution function of (2) is given by [2]

$$F_{\hat{\gamma}^2}(x \mid N, \gamma^2 = 0) = 1 - (1 - x)^{N-1} \tag{4}$$

for $0 \leqslant x \leqslant 1$, and the probability density function is

$$f_{\hat{\gamma}^2}(x \mid N, \gamma^2 = 0) = (N - 1)(1 - x)^{N-2} \tag{5}$$

for $0 \leqslant x \leqslant 1$, and N is the number of independent data segments. These follow from the fact that the $F_i(f; k)$ in (2) are complex Gaussian random variables [2].

(b) Signal present. In this case the true value of the MSC is assumed to be nonzero. The distribution function of (2) for nonzero true coherence is

$$F_{\hat{\gamma}^2}(x \mid N, \gamma^2) = x\left(\frac{1 - \gamma^2}{1 - x\gamma^2}\right)^N \sum_{k=0}^{N-2} \left(\frac{1 - x}{1 - x\gamma^2}\right)^k {}_2F_1(-k, 1 - N; 1; x\gamma^2) \tag{6}$$

and the density function is

$$f_{\hat{\gamma}^2}(x \mid N, \gamma^2) = (N - 1)(1 - \gamma^2)^N (1 - x)^{N-2} (1 - x\gamma^2)^{1-2N} \, {}_2F_1(1 - N, 1 - N; 1; x\gamma^2) \tag{7}$$

where ${}_2F_1(a, b; c; Z)$ is the Gaussian hypergeometric function defined by [3]

$${}_2F_1(a, b; c; Z) = \sum_{\ell=0}^{\infty} \frac{(a)_\ell (b)_\ell}{(c)_\ell} \frac{Z^\ell}{\ell!}$$

and $(a)_\ell$ is Pochhammer's symbol $(a)_\ell = \Gamma(a + \ell)/\Gamma(a)$, i.e.,

$$(a)_0 = 1$$

$$(a)_\ell = a(a + 1) \ldots (a + \ell - 1), \quad \ell = 1, 2, \ldots .$$

Note that when either a or b is a negative integer, then the ${}_2F_1$ function is simply a polynomial of finite degree. We also note that the distribution and density functions given in (4)

through (7) remain valid for the estimate given in (3) since the Fourier coefficients are, as noted after (3), complex Gaussian random variables.

3. DISTRIBUTION OF THE MAXIMUM

In this section we derive the distribution function of the maximum of the estimate of the magnitude squared coherence on a passive ambiguity surface. The estimates $\widehat{\gamma^2}(\tau, \theta)$ are assumed to be independent of each other and the total size of the surface is assumed to contain A points. Theorem 1 was originally obtained in [4].

Theorem 1. Let $Z_A = \max \{\widehat{\gamma^2}(\tau, \theta) : \tau \in T, \theta \in \Theta\}$ be the maximum over A independent estimates of the (noise only) MSC where the true coherence is assumed to be zero ($\gamma^2 = 0$) for all values of $\tau \in T$ and $\theta \in \Theta$ over which the maximum is taken. Then, the distribution function of Z_A is given by

$$F_{Z_A}(x \mid A, N, \gamma^2 = 0) = \begin{cases} 0, & x < 0, \\ \exp\left[-A(1-x)^{N-1}\right], & 0 \leq x \leq 1, \\ 1, & 1 < x, \end{cases} \tag{8}$$

and the density function is

$$f_{Z_A}(x \mid A, N, \gamma^2 = 0) = A(N-1)(1-x)^{N-2} \exp\left[-A(1-x)^{N-1}\right], \tag{9}$$

for $0 \leq x \leq 1$, and 0 otherwise.

Proof. The set of estimates $\{\widehat{\gamma^2}(\tau, \theta)\}$ are independent and identically distributed with the common distribution function (4). By [5, p. 36], Z_A has a type 3 asymptotic distribution given by (8) since $1 - F(x)$ behaves like $\beta(x_0 - x)^\alpha$ with $\beta = 1$, $x_0 = 1$, and $\alpha = N - 1$. That the density function is given by (9) follows immediately by differentiating (8). □

We note that if the distribution function (8) for Z_A is expanded into a Taylor series, then the first two terms of the series expansion gives the approximation

$$F_{Z_A}(x \mid A, N, \gamma^2 = 0) \simeq 1 - A(1-x)^{N-1}$$

which reduces to the distribution function of a single point (4) on the PAS for A = 1. Figure 1 presents graphs of (5) and (9) for various values of A when the true coherence is zero (i.e., noise only).

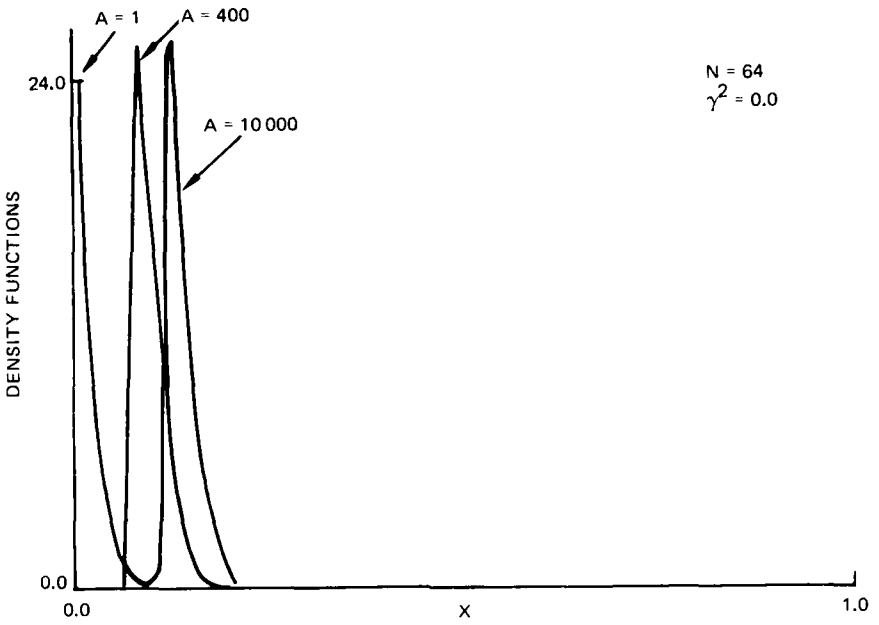

Figure 1. Density functi ns $f_{Z_A}(x \mid A, N, \gamma^2 = 0)$ for $Z_A = \max \widehat{\gamma^2}$, the maximum of the estimates o the MSC with noise only present. (Surface size = A; degrees of freedom = N; 'rue MSC = γ^2.)

We now turn to the case when a signal is present, that is, when one estimate is based on data with a true MSC of $\gamma^2 \neq 0$ and all of the other estimates on the surface have only noise present. Thus, one estimate of the MSC has a distribution function given by (6), while the remaining A–1 estimates on the surface have a distribution function given by (4). We now present

Theorem 2. Let $\underset{\sim}{Z}_A = \max \{ \widehat{\gamma^2}(\tau, \theta) : (\tau, \theta) \in T \times \Theta \}$ be the maximum over A independent estimates of $\widehat{\gamma^2}(\tau, \theta)$ where one estimate is distributed according to (6) and the remaining A–1 estimates are distributed according to (4). Then, the distribution function of $\underset{\sim}{Z}_A$ is

$$F_{\underset{\sim}{Z}_A}(x \mid A, N, \gamma^2) = \exp\left[-(A-1)(1-x)^{N-1}\right] \times \left(\frac{1-\gamma^2}{1-x\gamma^2}\right)^N$$

$$\sum_{k=0}^{N-2} \left(\frac{1-x}{1-x\gamma^2}\right)^k {}_2F_1(-k, 1-N; 1; x\gamma^2), \qquad (10)$$

for $0 \leq x < 1$. The density function is given by

$$f_{\underset{\sim}{Z}_A}(x \mid A, N, \gamma^2) = (N-1)\left(\frac{1-\gamma^2}{1-x\gamma^2}\right)^N (1-x)^{N-2}$$

$$\exp\left[-(A-1)(1-x)^{N-1}\right]\Bigg\{(1-x\gamma^2)^{1-N}\ {}_2F_1(1-N, 1-N; 1; x\gamma^2)$$

$$+ (A-1)x \sum_{k=0}^{N-2}\left(\frac{1-x}{1-x\gamma^2}\right)^k\ {}_2F_1(-k, 1-N; 1; x\gamma^2)\Bigg\}, \qquad (11)$$

for $0 \leq x \leq 1$.

Proof. Let τ_0 and θ_0 be the location on the surface where the true coherence γ^2 is nonzero. Then

$$\underset{\sim}{Z}_A = \max\left\{\widehat{\gamma^2}(\tau, \theta) : (\tau, \theta) \in T \times \Theta\right\}$$

$$= \max\left\{\widehat{\gamma^2}(\tau_0, \theta_0),\ Z_{A-1}\right\}$$

where

$$Z_{A-1} = \max\left\{\widehat{\gamma^2}(\tau, \theta) : (\tau, \theta) \in T \times \Theta \setminus \{(\tau_0, \theta_0)\}\right\}$$

and $T \times \Theta \setminus \{(\tau_0, \theta_0)\}$ is the set containing $A - 1$ points which excludes the point (τ_0, θ_0). Thus the distribution function of $\underset{\sim}{Z}_A$ is given by

$$F_{\underset{\sim}{Z}_A}(x \mid A, N, \gamma^2) = P_r\left\{\underset{\sim}{Z}_A \leq x\right\}$$

$$= P_r\left\{\widehat{\gamma^2}(\tau_0, \theta_0) \leq x,\ Z_{A-1} \leq x\right\}$$

$$= F_{\widehat{\gamma^2}}(x \mid N, \gamma^2)\, F_{Z_{A-1}}(x \mid A-1, N, \gamma^2 = 0)$$

which follows from the fact that $\widehat{\gamma^2}(\tau_0, \theta_0)$ is independent of the other estimates

$\left\{\widehat{\gamma^2}(\tau, \theta) : (\tau, \theta) \in T \times \Theta \setminus \{(\tau_0, \theta_0)\}\right\}$. The distribution function $F_{\widehat{\gamma^2}}(x \mid N, \gamma^2)$ is given by (4) and the distribution function $F_{Z_{A-1}}(x \mid A - 1, N, \gamma^2 = 0)$ is given by (8) of Theorem 1. The theorem now follows. □

We note that when A = 1, the extreme value distribution function of $\underset{\sim}{Z}_1$ given in (10) reduces to the distribution function of a single point (with a signal present) on the PAS as given in (6). Plots of the density functions (9) for a signal present are given in Figures 2 and 3 for various surface sizes and different numbers of degrees of freedom. Note that as the maximum is taken over more estimates on the surface the density function "shifts" to the right, as would be expected. Also note that when Figure 2 is compared to Figure 3, the density functions for an increased number of degrees of freedom N (Figure 3) have less "separation." Comparing Figures 1 and 2 shows the change between noise only and noise plus signal present.

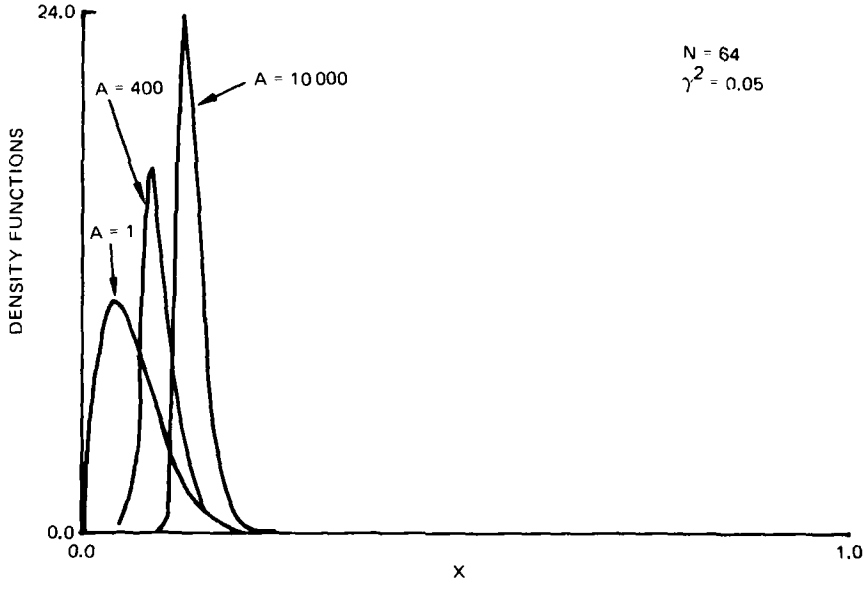

Figure 2. Density functions $f_{\underset{\sim}{Z}_A}(x \mid A, N, \gamma^2)$ for $\underset{\sim}{Z}_A = \max \widehat{\gamma^2}$, the maximum of the estimates of the MSC when a signal is present. (Surface size = A; degrees of freedom = N; true MSC = γ^2.)

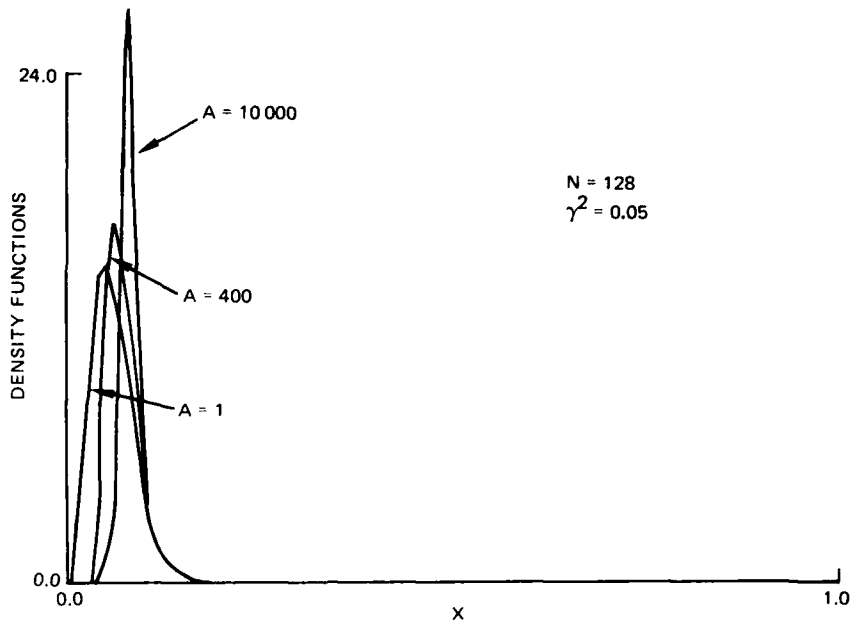

Figure 3. Density functions $f_{\underset{\sim}{Z}_A}(x \mid A, N, \gamma^2)$ for $\underset{\sim}{Z}_A = \max \hat{\gamma}^2$, the maximum of the estimates of the MSC when a signal is present. (Surface size = A; degrees of freedom = N; true MSC = γ^2.)

4. APPLICATIONS TO DETECTION STATISTICS

In this section we apply the results of Theorems 1 and 2 to the problem of signal detection on a passive ambiguity surface using the maximum (or peak) value on the surface as a detection statistic. We formulate a Neyman-Pearson hypotheses test and obtain expressions for the probability of false alarm and probability of detection in terms of the number of degrees of freedom N (i.e., the number of independent segments of data), the size of the passive ambiguity surface A, and the true coherence γ^2.

Let the observation of the maximum be

$$\zeta_A = \max\left\{\hat{\gamma}^2(\tau, \theta) : (\tau, \theta) \in T \times \Theta\right\} \quad ,$$

that is, ζ_A is the maximum value of the estimates of the MSC on a surface containing A points. The hypothesis H_0 of the Neyman-Pearson test is the case when no signal is present, which is characterized by a true coherence of $\gamma^2 = 0$ for each estimate on a PAS of size A. Under H_0

the observation $\zeta_A = Z_A$ is described by the density function (7) given in Theorem 1. The hypothesis H_1 is the case when a signal is present, i.e., the true coherence γ^2 is nonzero for one particular pair of (τ_0, θ_0) and is zero for the other A-1 points on the surface. In this case the observation $\zeta_A = \underset{\sim}{Z}_A$ and has the density function (9) of Theorem 2. Thus, the hypotheses test is

$$H_0 : \zeta_A = Z_A , \qquad p_0(x) = f_{Z_A}(x \mid A, N, \gamma^2 = 0) ;$$

$$H_1 : \zeta_A = \underset{\sim}{Z}_A , \qquad p_1(x) = f_{\underset{\sim}{Z}_A}(x \mid A, N, \gamma^2 \neq 0) .$$

The probability of false alarm and probability of detection are now readily calculated as

$$Q_0 = p_{F_A}(x_0) = \int_{x_0}^{1} p_0(x)\, dx$$

$$= 1 - F_{Z_A}(x_0 \mid A, N, \gamma^2 = 0)$$

and

$$Q_d = p_D(x_0) = \int_{x_0}^{1} p_1(x)\, dx$$

$$= 1 - F_{\underset{\sim}{Z}_A}(x_0 \mid A, N, \gamma^2)$$

where the distribution functions F_{Z_A} and $F_{\underset{\sim}{Z}_A}$ are given in (6) of Theorem 1 and, respectively, in (8) of Theorem 2. We note that in Neyman-Pearson type detection the probability of false alarm is set at some predetermined value. Solving for the threshold x_0 in terms of the probability of false alarm Q_0 gives

$$x_0 = 1 - \left[(-1/A)\,\ell n(1 - Q_0)\right]^{1/(n-1)} .$$

For the sake of comparison we also determine the detection performance of the MSC estimate for a single point [6] [7]. In this case the hypotheses are

$$H_0 : \zeta = \widehat{\gamma^2} , \qquad p_0(x) = f_{\widehat{\gamma^2}}(x \mid N, \gamma^2 = 0) ;$$

$$H_1 : \zeta = \underset{\sim}{\widehat{\gamma^2}} , \qquad p_1(x) = f_{\underset{\sim}{\widehat{\gamma^2}}}(x \mid N, \gamma^2 \neq 0) ,$$

where $f_{\hat{\gamma}^2}(x \mid N, \gamma^2 = 0)$ is given by (5) and $f_{\hat{\gamma}^2}(x \mid N, \gamma^2)$ is given by (7). The probability of false alarm and probability of detection are easily calculated as above.

The comparisons between the detection performance of the "peak" (or maximum) value of the estimates of the MSC on a PAS and a single estimate of the MSC are given in Figures 4 through 6. In these figures receiver operating characteristic (ROC) curves depict the detection performance. Figure 4 shows that the detection performance of the maximum decreases as the size of the surface increases (with the degrees of freedom N and true coherence γ^2 both fixed). Figure 5 indicates the expected result that the probability of detection increases as the true coherence increases. In Figure 6 the increase in the probability of detection when the number of degrees of freedom also is increased is indicated. We note that in the above figures the ROC curves for A = 1 can be obtained from [6].

Since the ROC curves presented in Figures 4 through 6 have a linear scale, the detection performance for small values of the probability of false alarm is difficult to determine. Thus, in Figures 7 through 9 the probability of detection is plotted against $10 \log_{10}(\gamma^2)$, where γ^2 is the true coherence and the probability of false alarm is fixed. Figure 7 again shows that the detection performance of the maximum degrades as the size of the surface increases. In Figure 8 we see that increasing the probability of false alarm also increases the probability of detection. Finally, the increase in the probability of detection as the number of degrees of freedom increases is indicated in Figure 9.

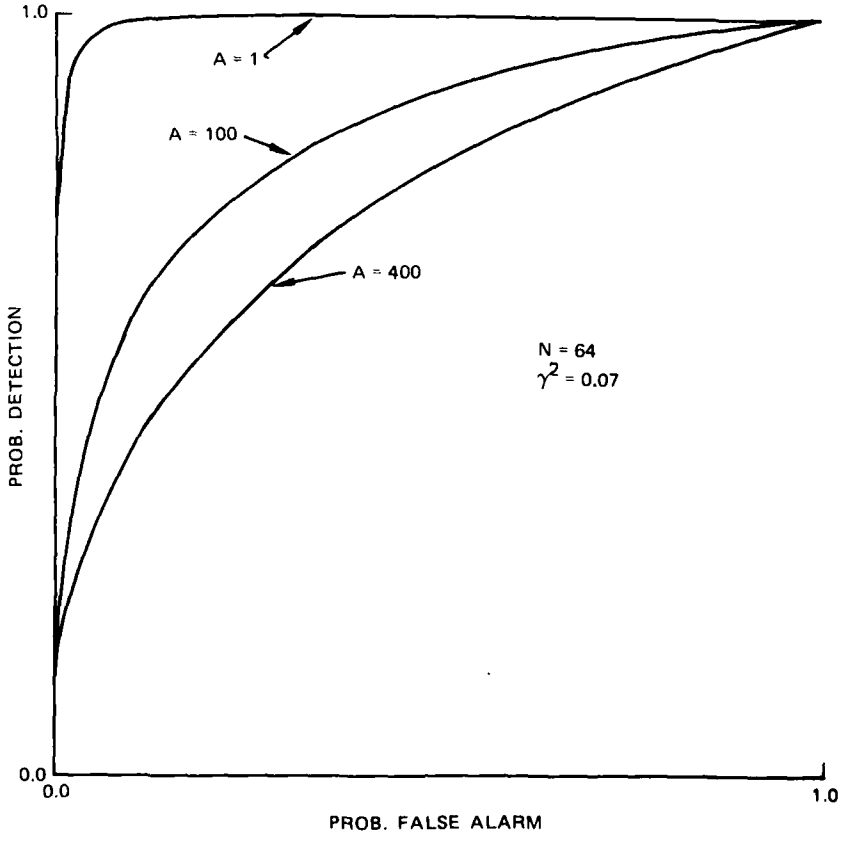

Figure 4. ROC curves for the detection statistic $\zeta_A = \max \hat{\gamma}^2$. (Surface size = A; degrees of freedom = N; true MSC = γ^2.)

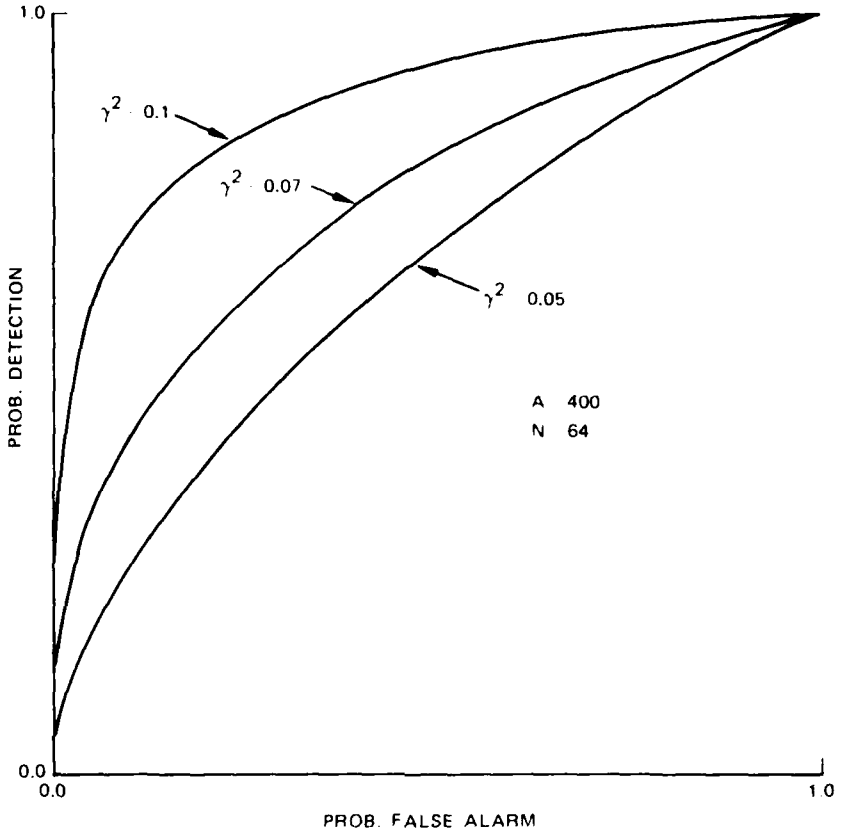

Figure 5. ROC curve for the detection statistic $\xi_A = \max \hat{\gamma}^2$. (Surface size = A; degrees of freedom = N; true MSC = γ^2.)

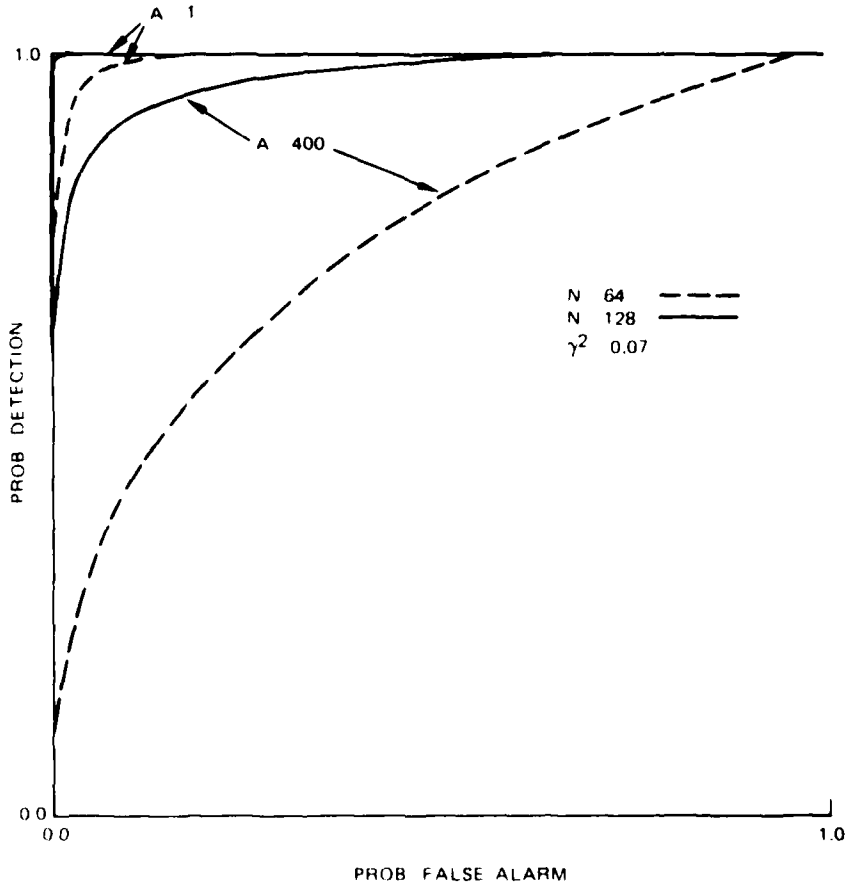

Figure 6. ROC curves for the detection statistic $\zeta_A = \max \hat{\gamma}^2$. (Surface size = A; degrees of freedom = N; true MSC = γ^2.)

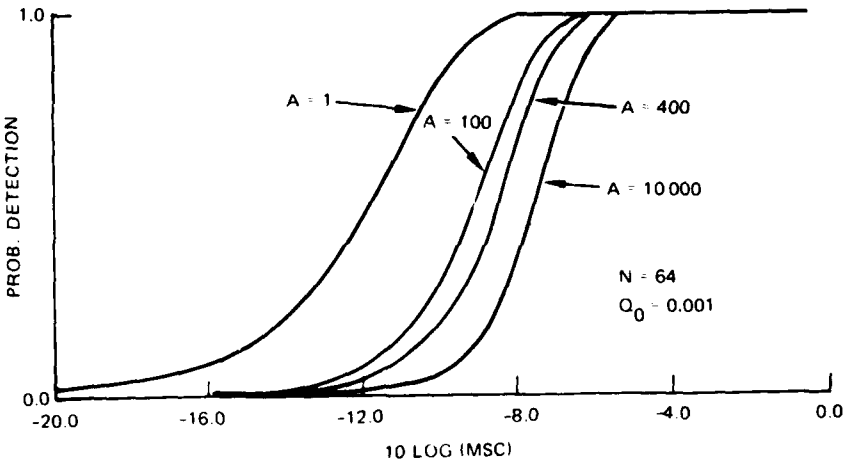

Figure 7. Detection curves for $\zeta_A = \max \hat{\gamma}$. (Surface size = A; degrees of freedom = N; probability of false alarm = Q_0.)

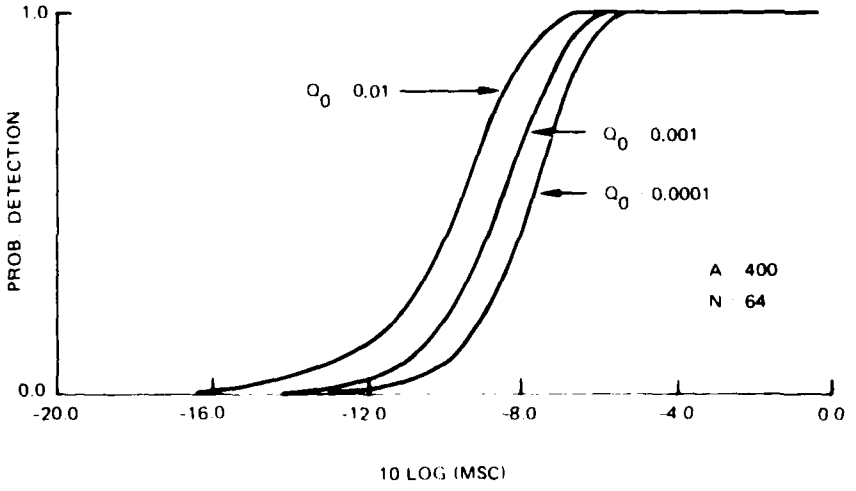

Figure 8. Detection curves for $\zeta_A = \max \hat{\gamma}$. (Surface size = A; degrees of freedom = N; probability of false alarm = Q_0.)

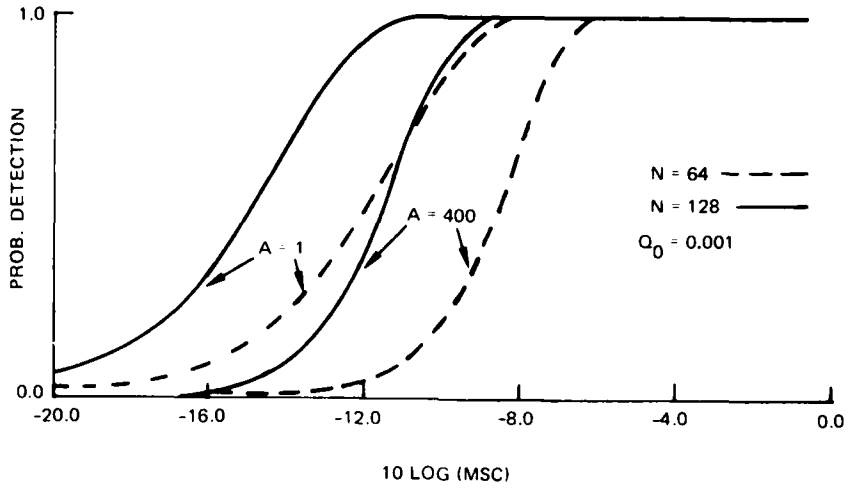

Figure 9. Detection curves for $\zeta_A = \max \hat{\gamma}^2$. (Surface size = A; degrees of freedom = N; Q_0 = probability of false alarm.)

5. EXTENSION TO MULTIPLE COHERENCE

The estimate of the magnitude-squared multiple coherence has also been considered as a detection statistic [7]. In this section we present a brief review of multiple coherence and derive the extreme value statistics of the maximum taken over estimates of the magnitude-squared multiple coherence. These results are then used to obtain the detection performance of the estimate of the magnitude-squared multiple coherence.

We let p designate the number of source channels receiving measurements. In particular, the case of p = 2 reduces to the magnitude-squared coherence (MSC) studied in Sections 2 and 3. Let $X(t) = (X_1(t), \ldots, X_p(t))^T$ be a real, zero mean, Gaussian vector random process which is wide-sense stationary. The correlation matrix is defined by

$$R(t) = \left[\!\left[E\, X_j(s+t)\, X_k(s) \right]\!\right] = \left[\!\left[R_{jk}(t) \right]\!\right]$$

where $\left[\!\left[R_{jk}(t) \right]\!\right]$ is the p by p matrix with elements $R_{jk}(t)$. The associated power spectral densities are assumed to exist with

$$\phi_{jk}(f) = \int_{-\infty}^{\infty} R_{jk}(t) \exp(-i 2\pi f t)\, dt$$

for $1 \leq j, k \leq p$, and $\phi(f)$ is the spectral density matrix

$$\phi(f) = \left[\left[\phi_{jk}(f)\right]\right] .$$

The magnitude-squared multiple coherence (MSMC) is defined in terms of the power spectral density matrix $\phi(f)$ and its inverse $\phi^{-1}(f)$ where the elements of $\phi^{-1}(f)$ are designated by

$$\phi^{-1}(f) = \left[\left[\phi^{jk}(f)\right]\right] .$$

The MSMC $\mu^2_{j \cdot 1, 2, \ldots, j-1, j+1, \ldots, p}$ of the j^{th} channel is defined by

$$\mu^2_{j \cdot 1, \ldots, j-1, j+1, \ldots, p}(f) = 1 - 1 \left[\phi_{jj}(f)\, \phi^{jj}(f)\right] \qquad (12)$$

for $j = 1, \ldots, p$. We note that the MSMC can be obtained inductively in terms of the pairwise complex coherence (not magnitude-squared coherence) as indicated in [8]. We also note that when $p = 2$, the MSMC $\mu^2_{1 \cdot 2}(f)$ (or $\mu^2_{2 \cdot 1}(f)$) reduces to the MSC $\gamma^2(f)$ defined in (1) and

$$\mu^2_{1 \cdot 2}(f) = \mu^2_{2 \cdot 1}(f) = \gamma^2(f) .$$

For notational convenience we designate the MSMC as μ^2 (or $\mu^2_j(f)$) and suppress the dependence on j, p, and f (or, respectively, p).

The MSMC estimate $\hat{\mu}^2_j(f)$ is formed from an estimate of the spectral density matrix $\hat{\phi}(f) = \left[\left[\hat{\phi}_{jk}(f)\right]\right]$ and its inverse $\left[\hat{\phi}(f)\right]^{-1} = \left[\left[\hat{\phi}^{jk}(f)\right]\right]$. The MSMC estimate is given by

$$\widehat{\mu^2_j}(f) = 1 - 1 \left[\hat{\phi}_{jj}(f)\, \hat{\phi}^{jj}(f)\right]$$

When a signal is absent, i.e., the true MSMC is zero, the distribution of the MSMC estimate $\widehat{\mu^2}$ is given by [2]

$$1 - \widehat{\mu^2}(N, p, N, \mu^2 = 0)$$

$$= 1 - (N - 1 + p)\binom{N-1}{p-2} \sum_{\ell=0}^{p-2} \frac{(-1)^\ell}{N - p + \ell + 1} \binom{p-2}{\ell} (1 - x)^{N-p+\ell+1} . \qquad (13)$$

and the density function is

$$f_{\widehat{\mu^2}}(x \mid p, N, \mu^2 = 0) = \frac{\Gamma(N)}{\Gamma(p-1)\,\Gamma(N-p+1)}\, x^{p-2}(1-x)^{N-p} \quad . \tag{14}$$

For the case of a signal present, the distribution is given by [2] [9]

$$F_{\widehat{\mu^2}}(x \mid p, N, \mu^2) = x^{p-1}\left(\frac{1-\mu^2}{1-x\mu^2}\right)^N \sum_{k=0}^{N-p} \frac{(p-2+k)!}{(p-2)!\,k!}$$

$$\left(\frac{1-x}{1-x\mu^2}\right)^k \; {}_2F_1(-k, p-1-N; p-1; x\mu^2) \tag{15}$$

and the density function is

$$f_{\widehat{\mu^2}}(x \mid p, N, \mu^2) = \frac{\Gamma(N)\,(1-\mu^2)^N\, x^{p-2}(1-x)^{N-p}}{\Gamma(p-1)\,\Gamma(N-p+1)\,(1-x\mu^2)}\, 2N-p+1$$

$${}_2F_1(p-1-N, p-1-N; p-1; x\mu^2) \quad . \tag{16}$$

The following two theorems for the magnitude-squared multiple coherence extend Theorems 1 and 2:

Theorem 1'. Let $\mu Z_A = \max\left\{\hat{\mu}^2(\tau, \theta) : (\tau, \theta) \in T \times \Theta\right\}$ be the maximum over A independent estimates of the MSMC and assume that the true multiple coherence for each estimate is 0 (i.e., $\mu^2 = 0$). Then the distribution function of μZ_A is

$$F_{\mu Z_A}(x \mid A, p, N, \mu^2 = 0)$$

$$= \begin{cases} 0, & x < 0, \\ \exp\left[-A\binom{N-1}{p-2}(1-x)^{N-p+1}\right], & 0 \leq x \leq 1, \\ 1, & 1 < x, \end{cases} \tag{17}$$

and the density function is

$$f_{\mu Z_A}(x \mid A, p, N, \mu^2 = 0)$$

$$= A\binom{N-1}{p-2}(N-p+1)(1-x)^{N-p} \exp\left[-A\binom{N-1}{p-2}(1-x)^{N-p+1}\right], \quad (18)$$

for $0 \leq x \leq 1$, and 0 otherwise.

Proof. As in Theorem 1, μZ_A has a type 3 asymptotic distribution [5] since

$$1 - F_{\hat{\mu}^2}(x \mid p, N, \mu^2 = 0) = \binom{N-1}{p-2}(1-x)^{N-p+1} + o\left[(1-x)^{N-p+1}\right]$$

as $x \to 1$. The theorem now follows from the independence of the A estimates for the MSMC. □

Again we note that Theorem 1 is a special case of Theorem 1′ when $p = 2$. We now proceed to the case of a signal present in one of the estimates:

Theorem 2′. Let $\mu \underset{\sim}{Z}_A = \max\left\{\hat{\mu}^2(\tau, \theta) : (\tau, \theta) \in T \times \Theta\right\}$ be the maximum over A independent estimates of the MSMC where one estimate is distributed according to (15) and the remaining A–1 estimates are distributed according to (13). Then the distribution function of $\mu \underset{\sim}{Z}_A$ is

$$F_{\mu \underset{\sim}{Z}_A}(x \mid A, p, N, \mu^2)$$

$$= \exp\left[-(A-1)\binom{N-1}{p-2}(1-x)^{N-p+1}\right] x^{p-1}\left(\frac{1-\mu^2}{1-x\mu^2}\right)^N$$

$$\sum_{k=0}^{N-p} \frac{(p-2+k)!}{(p-2)!\,k!}\left(\frac{1-x}{1-x\mu^2}\right)^k {}_2F_1(-k, p-1-N; p; x\mu^2) \quad (19)$$

for $0 \leq x \leq 1$. The density function is

$$f_{\mu \underset{\sim}{Z}_A}(x \mid A, p, N, \mu^2)$$

$$= \frac{\Gamma(N)\, x^{p-2}(1-x)^{N-p}}{\Gamma(p-1)\,\Gamma(N-p+1)}\left(\frac{1-\mu^2}{1-x\mu^2}\right)^N \exp\left[-(A-1)\binom{N-1}{p-2}(1-x)^{N-p+1}\right]$$

$$\Bigg\{(1-x\mu^2)^{p-1-N}\,{}_2F_1(p-1-N,\,p-1-N;\,p-1;\,x\mu^2)$$

$$+(A-1)\,x\,(1-x)^{p-2}\sum_{k=0}^{N-p}\frac{(p-2+k)!}{(p-2)!\,k!}\left(\frac{1-x}{1-x\mu^2}\right)^k$$

$$\times\,{}_2F_1(-k,\,p-1-N;\,p-1;\,x\mu^2)\Bigg\} \tag{20}$$

for $0 \leq x \leq 1$.

Proof. Proceeding as in the proof of Theorem 2, we obtain

$$F_{\mu\underset{\sim}{Z}_A}(x \mid A, p, N, \mu^2) = F_{\widehat{\mu^2}}(x \mid p, N, \mu^2)\, F_{\mu Z_{A-1}}(x \mid A-1, p, N, \mu^2 = 0)$$

and the theorem now follows directly from (17) of Theorem 1′ and (15). □

Plots of the density functions $f_{\mu Z_A}(x \mid A, p, N, \mu^2 = 0)$ and $f_{\mu\underset{\sim}{Z}_A}(x \mid A, p, N, \mu^2)$ are given in Figures 10 through 14. Figure 10 shows plots of the density function (18) when only noise is present. (See Figure 1 for the case $p = 2$.) In Figure 11, the effect of increasing the number of source channels p is shown. The effect of increasing the surface size A is shown in Figure 12; also, the effect of changing the number of source channels p is contrasted between Figure 12a and 12b. The effect of changing the true multiple coherence μ^2 is indicated in Figure 13. Finally, Figure 14 indicates the result of changing the number of degrees of freedom.

As in the case of the MSC estimates which form a passive ambiguity surface, Neyman-Pearson type signal detection hypotheses can be formulated by using the maximum value of the estimate of magnitude-squared multiple coherence as a detection statistic. In this case, the measurement

$$\mu\zeta_A = \max\left\{\widehat{\mu^2}(\tau, \theta) : (\tau, \theta) \in T \times \Theta\right\}$$

has either the distribution under H_0 defined by

$$H_0 : \mu\zeta_A = \mu Z_A \,,\; p_0(x) = f_{\mu Z_A}(x \mid A, p, N, \mu^2 = 0)$$

or, under H_1, when a signal is present

$$H_1 : \mu\zeta_A = \mu\underset{\sim}{Z}_A \,,\; p_1(x) = f_{\mu\underset{\sim}{Z}_A}(x \mid A, p, N, \mu^2)\,,$$

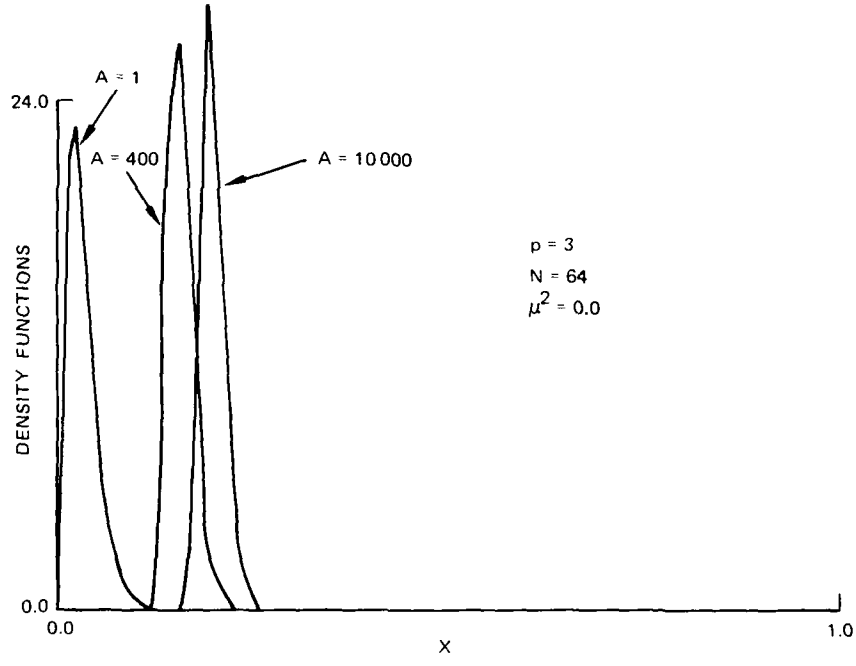

Figure 10. Density functions $f_{\mu Z_A}(x \mid A, p, N, \mu^2 = 0)$ for $\mu Z_A = \max \widehat{\mu^2}$, the maximum of the estimates of the MSMC with noise only present. (Surface size = A; degrees of freedom = N; number of channels = p; true MSMC = μ^2.)

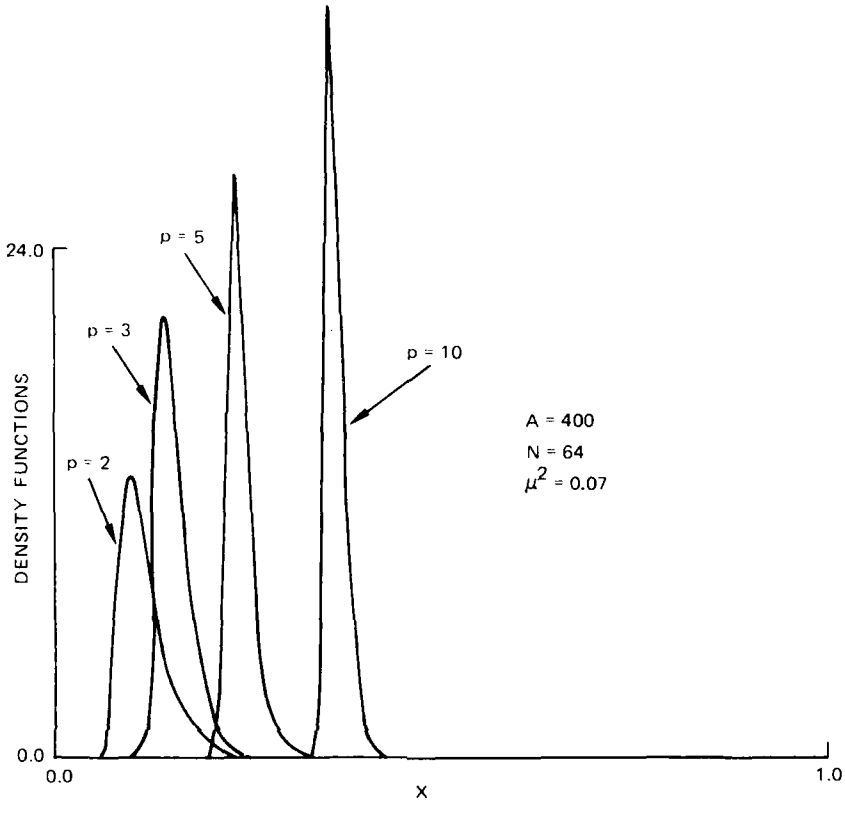

Figure 11. Density functions $f_{\mu\underset{\sim}{Z}_A}(x \mid A, p, N, \mu^2)$ for $\mu\underset{\sim}{Z}_A$, the maximum of the estimates of the MSMC when a signal is present. (Surface size = A; degrees of freedom = N; number of channels = p; true MSMC = μ^2.)

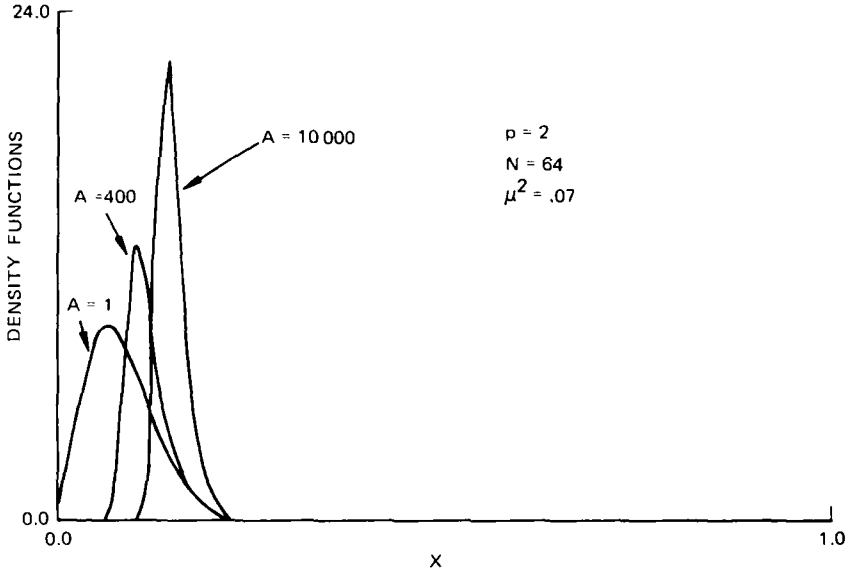

Figure 12a. Density functions for $\mu\underset{\sim}{Z}_A$ ($\underset{\sim}{Z}_A$), the maximum of the estimate of the MSMC (MSC) when a signal is present. Since p = 2, $\mu^{\sim 2} = \gamma^{\sim 2}$ and $\mu\underset{\sim}{Z}_A = \underset{\sim}{Z}_A$. (Surface size = A; degrees of freedom = N; number of channels = p; true MSMC = $\mu^{\sim 2}$.)

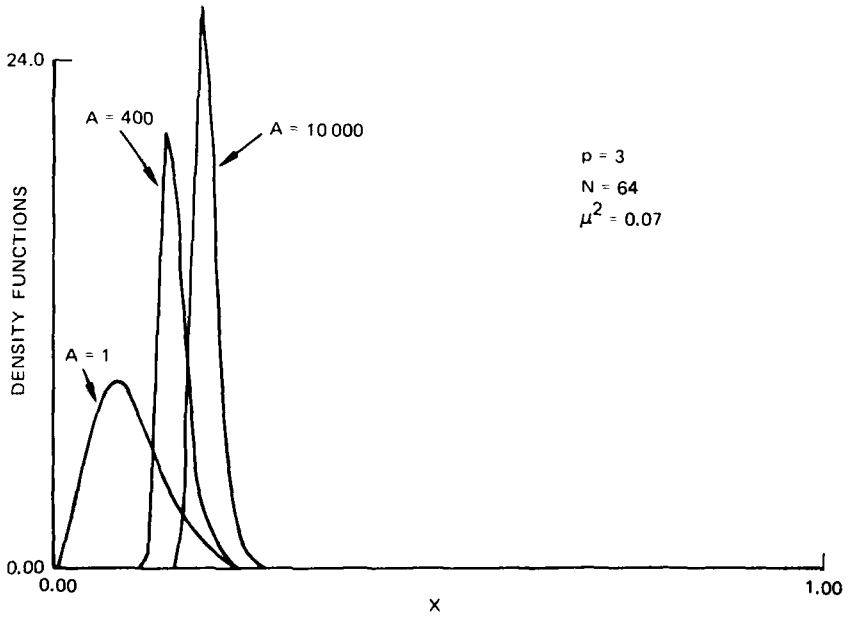

Figure 12b. Density functions for $\mu\underset{\sim}{Z}_A$, the maximum of the estimate of the MSMC when a signal is present. (Surface size = A; degrees of freedom = N; number of channels = p; true MSMC = $\mu^{\sim 2}$.)

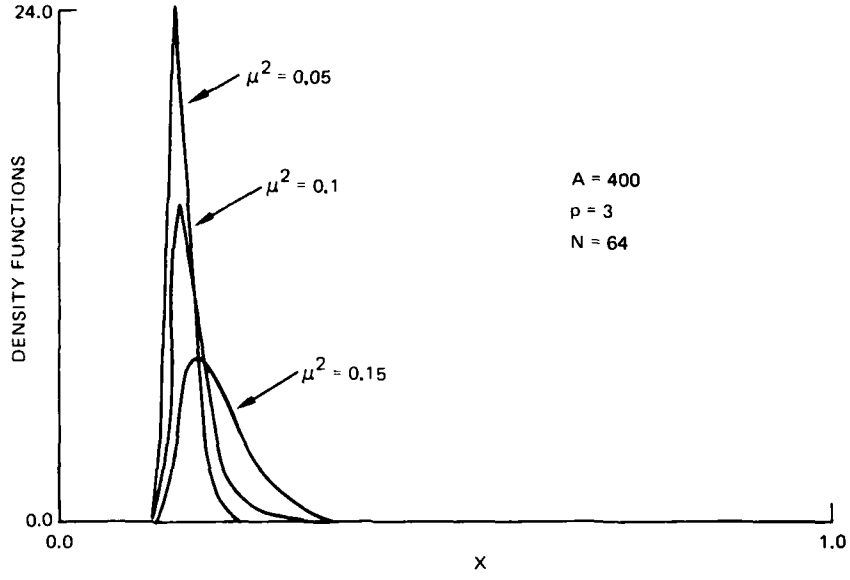

Figure 13. Density functions $f_{\mu\underset{\sim}{Z}_A}(x \mid A, p, N, \mu^2)$ for $\mu\underset{\sim}{Z}_A$, the maximum of the MSMC estimates when a signal is present. (Surface size = A; degrees of freedom = N; *number of channels* = p; *true MSMC* = μ^2.)

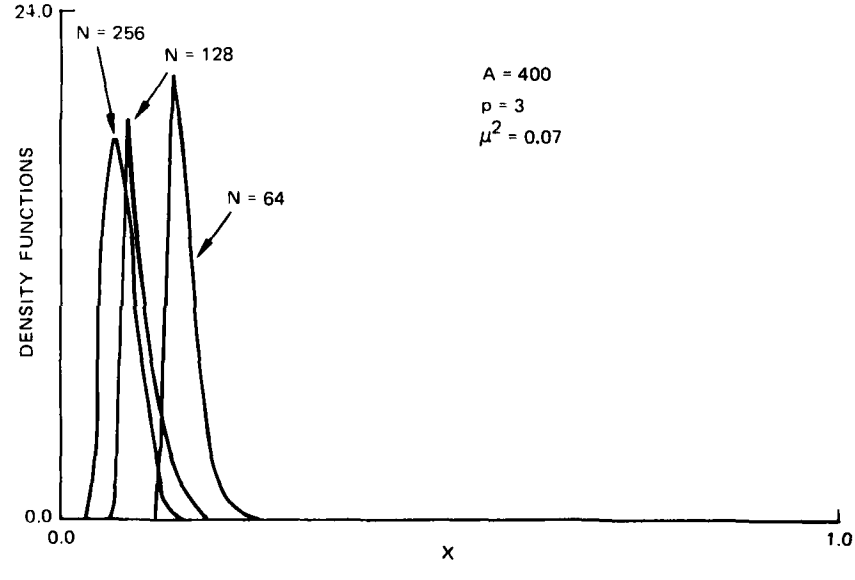

Figure 14. Density functions $f_{\mu\underset{\sim}{Z}_A}(x \mid A, p, N, \mu^2)$ for $\mu\underset{\sim}{Z}_A$, the maximum of the estimates of the MSMC when a signal is present. (Surface size = A; degrees of freedom = N; number of channels = p; true MSMC = μ^2.)

where $f_{\mu Z_A}$ and $f_{\mu \underset{\sim}{Z}_A}$ are given by (18) and (20), respectively. The probability of false alarm and probability of detection, for the maximum estimate of the MSMC, are given by

$$Q_0 = 1 - F_{\mu Z_A}(x_0 \mid A, p, N, \mu^2 = 0)$$

$$Q_d = 1 - F_{\mu \underset{\sim}{Z}_A}(x_0 \mid A, p, N, \mu^2)$$

where $F_{\mu Z_A}$ is given by (17) and $F_{\mu \underset{\sim}{Z}_A}$ is given by (19). The probabilities of false alarm and detection for a single estimate of the MSMC are also easily calculated as

$$Q_0 = 1 - F_{\hat{\mu}^2}(x_0 \mid p, N, \mu^2 = 0)$$

$$Q_d = 1 - F_{\hat{\underset{\sim}{\mu}}^2}(x_0 \mid p, N, \mu^2)$$

where $F_{\hat{\mu}^2}$ and $F_{\hat{\underset{\sim}{\mu}}^2}$ are given by (13), and respectively, (15).

The ROC curves for the peak value of the MSMC are presented in Figures 15 through 18. The curves for A = 1 can be obtained from [7]. In Figure 15 the effects of increasing the number of source channels p is shown to decrease the probability of detection. (See the discussion in Section 6.) Also, the effects of increasing the number of estimates A over which the maximum is taken, i.e., increasing the surface size, are again shown to decrease the probability of detection; this is clearly demonstrated in Figure 16. In Figure 15, the effect of increasing the true multiple coherence μ^2 is shown to increase the probability of detection. The effect of increasing N (the number of degrees of freedom) is shown in Figure 16 to increase the probability of detection.

Figures 19 through 22 are graphs of the probability of detection versus $10 \log_{10}$ (MSMC) when the probability of false alarm is fixed. Figure 19 shows that the effect of increasing the number of source channels p results in a decrease in the probability of detection (again, see the discussion in Section 6). The effect of increasing the surface size A is shown in Figure 20 – the probability of detection decreases. Figure 21 shows the expected result that the probability of detection decreases as the probability of false alarm decreases. Finally, we see in Figure 22 that increasing the number of degrees of freedom increases the probability of detection.

We conclude by addressing the fact that the probability of detection decreases as the number of source channels p increases under the assumption that the numerical value of the multiple coherence remains fixed. This is, perhaps, difficult to understand since the basic definition of multiple coherence changes as the number of source channels changes. As indicated in [7], the signal-to-noise ratio (SNR) in the individual channels must decrease in order that the "multiple coherence" stays constant when the number of source channels increases (under the assumption of equal SNR in all channels). However, this is only a partial explanation.

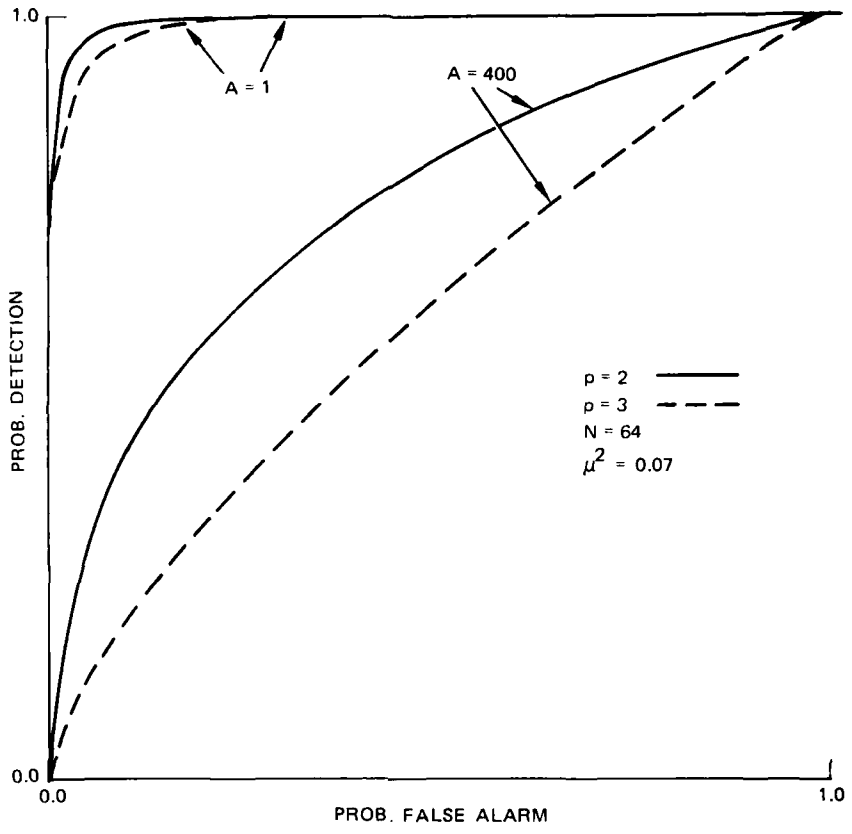

Figure 15. ROC curves for the magnitude-squared multiple coherence detection statistic $\mu\hat{\zeta}_A = \max \hat{\mu^2}$. (Surface size = A; degrees of freedom = N; number of channels = p; true MSMC = μ^2.)

To better understand multiple coherence we compare the following two cases that are based on the assumption that the SNR in the individual channels are equal. The equal SNR in each channel implies that the magnitude-squared multiple coherence (μ_p for p channels) and SNR (denoted R) are related by [7]

$$\mu_p^2 = \frac{(p-1)R^2}{(1+R)(1+(p-1)R)} \quad . \tag{21}$$

For case 1, let p = 2 and $\mu_2^2 = 0.07$ (= γ^2). From (21) we have that R = 0.359 (= SNR). For case 2, let p = 3 and let the SNR be as determined above, R = 0.359. Thus the magnitude-squared multiple coherence is equal to $\mu_3^2 = 0.11$. We now compare case 1 where p = 2 and $\mu_2^2 = 0.07$ with case 2 where p = 3 and $\mu_3^2 = 0.11$. The comparison is given in Figure 23, where the expected result of an increase in the probability of detection occurs when the SNR in the individual channels is held constant and the number of channels is increased.

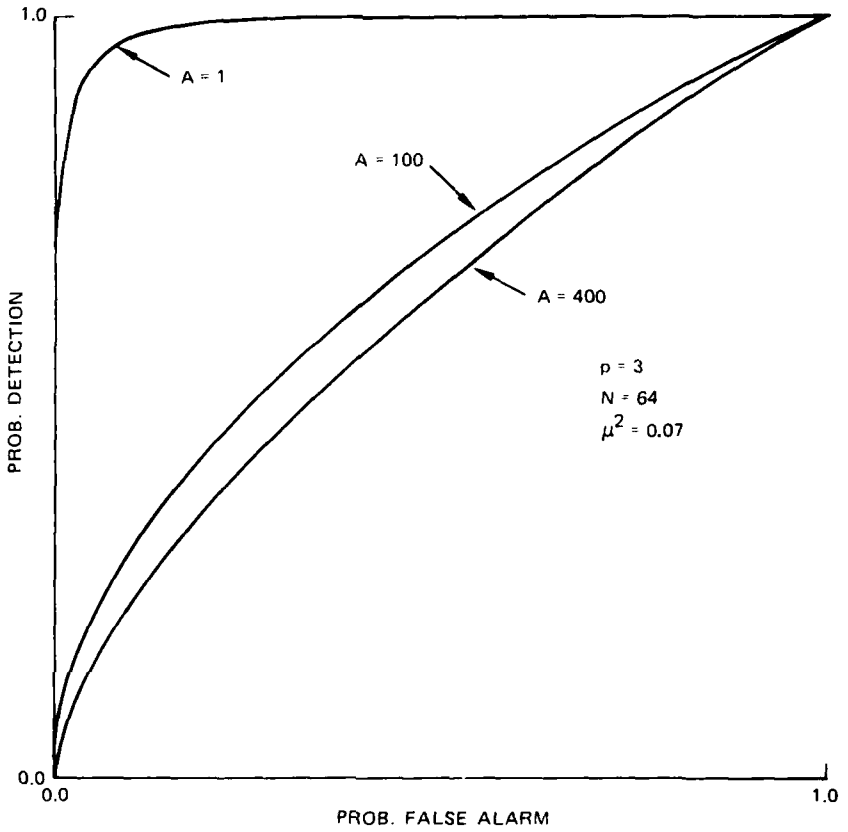

Figure 16. ROC curves for the magnitude-squared multiple coherence detection statistic $\mu\hat{\zeta}_A = \max \hat{\mu^2}$. (Surface size = A; degrees of freedom = N; number of channels = p; true MSMC = μ^2.)

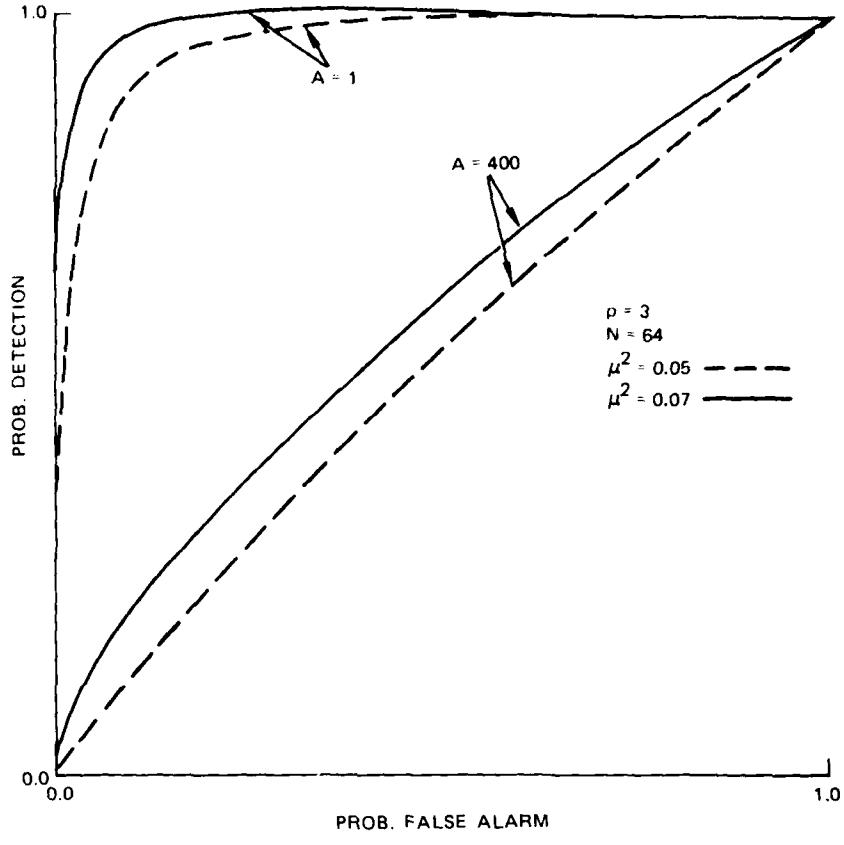

Figure 17. ROC curves for the magnitude-squared multiple coherence detection statistic $\mu\zeta_A = \max \hat{\mu^2}$. (Surface size = A; degrees of freedom = N; number of channels = p; true MSMC = μ^2.)

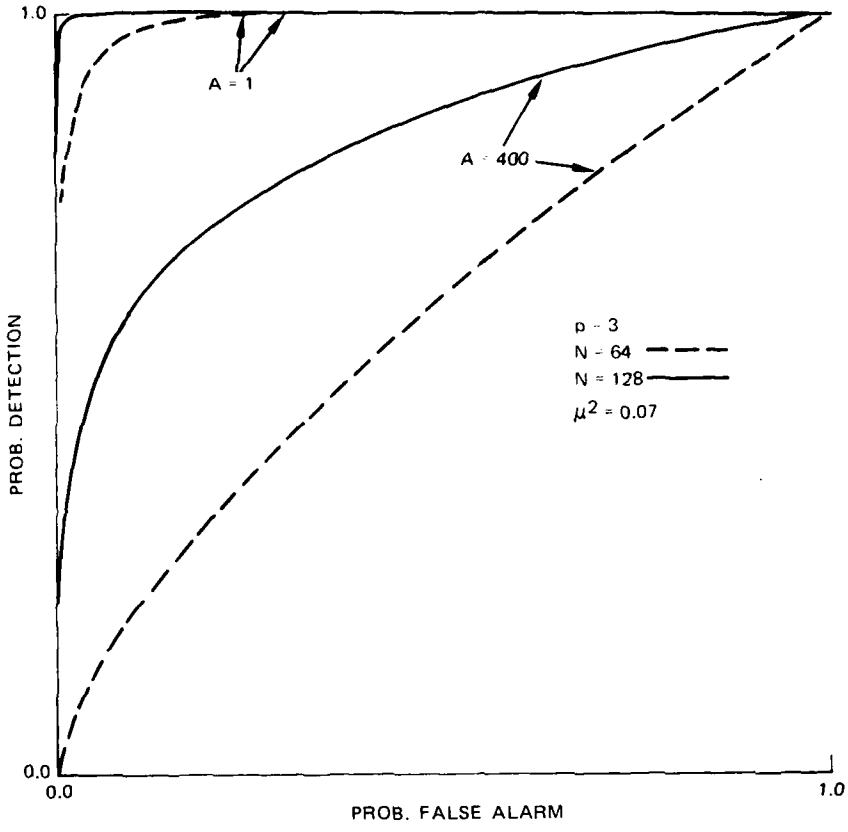

Figure 18. ROC curves for the magnitude-squared multiple coherence detection statistic $\mu\zeta_A = \max \widehat{\mu^2}$. (Surface size = A; degrees of freedom = N; number of channels = p; true MSMC = μ^2.)

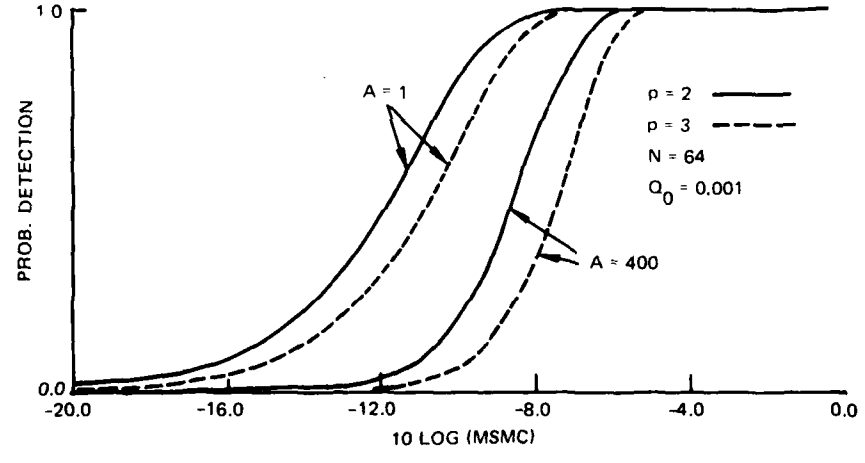

Figure 19. Detection curves for the magnitude-squared multiple coherence detection statistic $\mu\zeta_A = \max \mu\widehat{\gamma^2}$. (Surface size = A; degrees of freedom = N; probability of false alarm = Q_0; number of channels = p.)

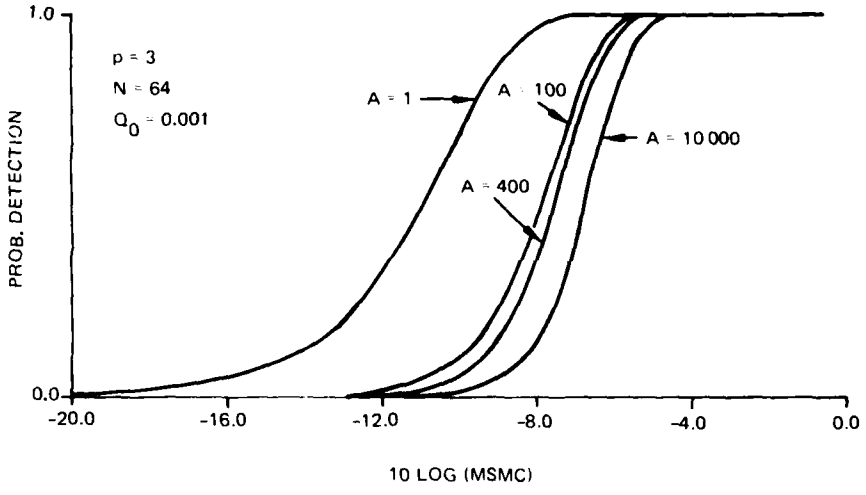

Figure 20. Detection curves for the magnitude-squared multiple coherence detection statistic $\mu\zeta_A = \max \widehat{\mu^2}$. (Surface size = A; degrees of freedom = N; probability of false alarm = Q_0; number of channels = p.)

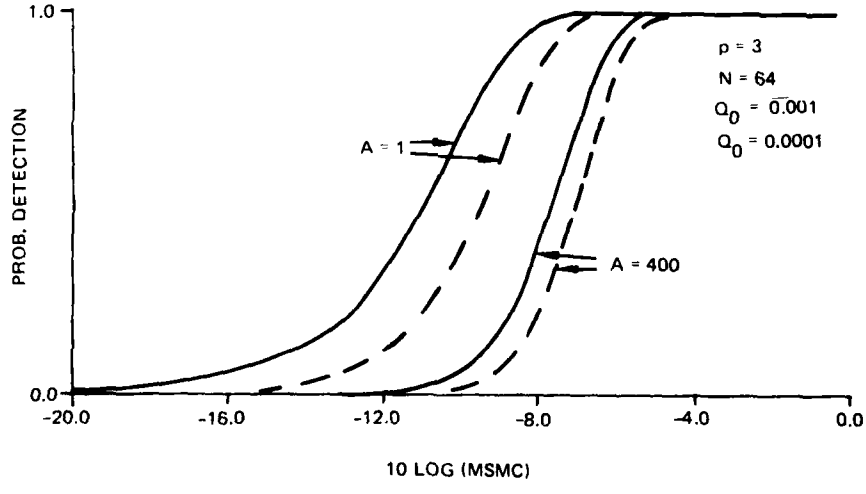

Figure 21. Detection curves for the magnitude-squared multiple coherence detection statistic $\mu\zeta_A = \max \widehat{\mu^2}$. (Surface size = A; degrees of freedom = N; probability of false alarm = Q_0; number of channels = p.)

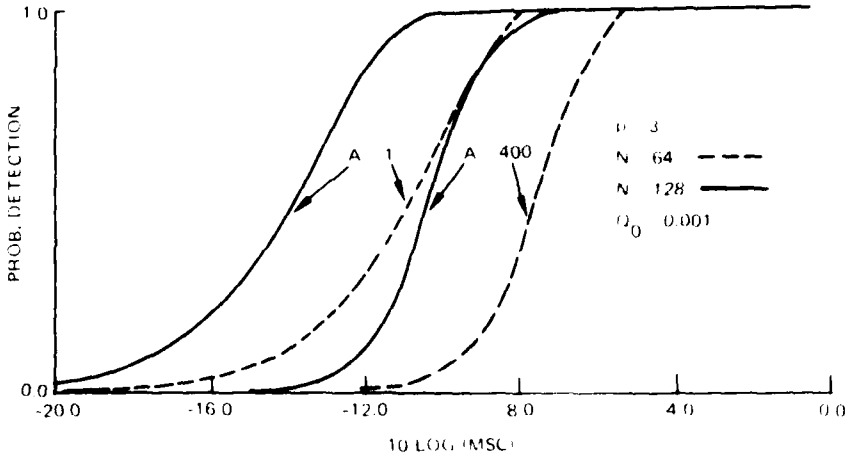

Figure 22. Detection curves for the magnitude-squared multiple coherence $\mu\zeta_A = \max \widehat{\mu^2}$ (Surface size = A; degrees of freedom = N; probability of false alarm = Q_0; number of channels = p.)

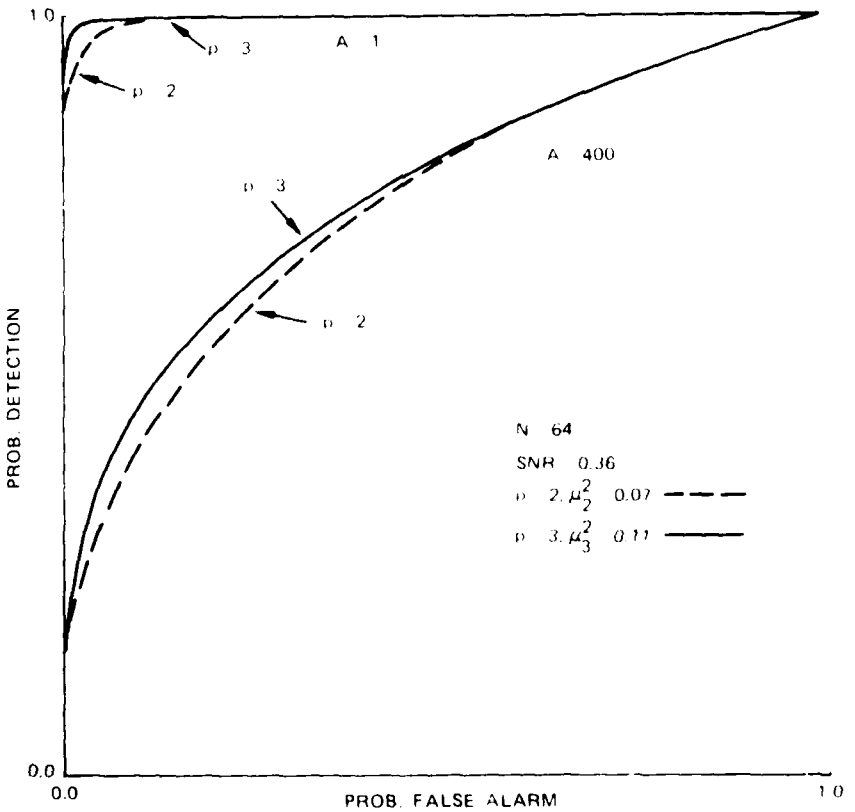

Figure 23. ROC curves for the magnitude-squared multiple coherence detection statistic $\mu\zeta_A = \max \widehat{\mu^2}$ with constant signal-to-noise-ratio. (Surface size = A; degrees of freedom = N; number of channels = p; true MSC with equal SNR = μ_2^2; true MSMC with equal SNR = μ_3^2.)

6. CONCLUSIONS

The performance of the extremum (or peak) on a passive ambiguity surface as a detection statistic has been derived in Section 4 for the case of magnitude-squared coherence and, in Section 5, for the case of the magnitude-squared multiple coherence. The following conclusions, valid for both cases, can be drawn:

(1) The probability of detection decreases as the size of the surface increases. An intuitive explanation of this behavior is that as the size of the surface is increased, more noise is "added" into the observation $\zeta_A = \text{Max}\ \hat{\gamma}^2$ (or, in the case of multiple coherence, $\mu\zeta_A = \text{Max}\ \hat{\mu}^2$). This is a direct consequence of the assumption that a signal is present in only one of the estimates while the other estimates are based on observations which contain noise only. Thus increasing the surface size A implies that only noisy data are incorporated into the measurement and that no contribution of signal information is made. As a consequence, the surface size should be chosen to be as small as possible but yet large enough to ensure that the signal is contained within the surface.

(2) The probability of detection increases as the true coherence γ^2 increases (or as the true multiple coherence μ^2 increases). This is an expected result which holds true in the case of a single estimate as indicated in [7].

(3) The probability of detection increases as the number of degrees of freedom N increases (or as the number of discrete Fourier transforms averaged to obtain an estimate increases). Again this is an expected result which also holds true for the single estimate [6] [7].

(4) The probability of detection increases as the number of source channels is increased, under the assumption that the signal-to-noise-ratio is the same in each of the individual channels. On the other hand, the probability of detection decreases as the number of source channels is increased, under the assumption that the multiple coherence is fixed

7. GLOSSARY

ABBREVIATIONS

MSC	Magnitude-squared coherence
MSMC	Magnitude-squared multiple coherence
PAS	Passive ambiguity surface
ROC	Receiver operating characteristics
SNR	Signal-to-noise ratio

SYMBOLS

$(a)_k$	Pochhammer's symbol
A	Size of the ambiguity surface
${}_2F_1$	Gauss' hypergeometric function
$F_i(f, k)$	The Fourier coefficient at the frequency f from the k^{th} discrete Fourier transform (DFT) of the process $x_i(t)$
$F_{\widehat{\gamma^2}}(x \mid N, \gamma^2 = 0)$	Distribution function of the MSC estimate when the true coherence is zero (signal absent)
$F_{\widehat{\gamma^2}}(x \mid N, \gamma^2)$	Distribution function of the MSC estimate when the true coherence is nonzero (signal present)
$F_{\mathcal{Z}_A}(x \mid A, N, \gamma^2 = 0)$	Distribution function of the maximum over MSC estimates when the true coherence is zero (signal absent)
$F_{\mathcal{Z}_A}(x \mid A, N, \gamma^2)$	Distribution function of the maximum over MSC estimates when the true coherence is nonzero (signal present)
$F_{\widehat{\mu^2}}(x \mid p, N, \mu^2 = 0)$	Distribution function of the MSMC estimate when the true multiple coherence is zero (signal absent)
$F_{\widehat{\mu^2}}(x \mid p, N, \mu^2)$	Distribution function of the MSMC estimate when the true multiple coherence is nonzero (signal present)
$F_{\mu\mathcal{Z}_A}(x \mid A, p, N, \mu^2 = 0)$	Distribution function of the maximum over MSMC estimates when the true coherence is zero (signal absent)
$F_{\mu\mathcal{Z}_A}(x \mid A, p, N, \mu^2)$	Distribution function of the maximum over MSMC estimates when the true coherence is nonzero (signal present)
$\gamma^2(f), \hat{\gamma}^2(f)$	Magnitude-squared coherence (and its estimate)
$\gamma^2(f, \tau, \theta), \hat{\gamma}^2(f, \tau, \theta)$	Magnitude-squared coherence corrected for time delay and doppler (and its estimate)
$\gamma^2(\tau, \theta), \hat{\gamma}^2(\tau, \theta)$	Same as the above with the frequency f suppressed
$\mu^2_{i \cdot 1, \ldots, i-1, i+1, \ldots, p}(f)$	Multiple coherence of channel i compared to the other p-1 channels
$\mu\mathcal{Z}_A$	Maximum over A estimates of the MSMC when no signal is present

$\mu\underline{Z}_A$	Maximum over A estimates of the MSMC when a signal is present
$\mu\underline{\zeta}_A$	The measurement over the maximum of A estimates of the MSMC
μ_p^2	The MSMC when the SNR is equal in all channels
N	Degrees of freedom (or the number of independent samples) in the MSC or MSMC estimate
p	Number of channels
$\phi_{jk}(f)$, $\hat{\phi}_{jk}(f)$	Cross-spectral density between channel j and channel k (or auto-spectral density when j=k) and its estimate
$\underline{\phi}(f)$, $\hat{\underline{\phi}}(f)$	Cross-spectral density matrix with elements $\phi_{jk}(f)$ and its estimate
Q_d	Probability of detection
Q_0	Probability of false alarm
$R_{jk}(t)$	Cross-correlation function between channel j and channel k (or auto-correlation function when j=k)
$\underline{R}(t)$	Cross-correlation matrix with elements $R_{ij}(t)$
T	Set of time delays at which MSC estimates are calculated
Θ	Set of doppler shifts at which MSC estimates are calculated
$x_i(t)$	Data in channel i
$\underline{x}(t)$	Vector of data $(x_1(t), \ldots x_p(t))^T$
$\underline{Z}_A$	Maximum over A estimates of the MSC when no signal is present
$\underline{Z}_A$	Maximum over A estimates of the MSC when a signal is present
ζ	The measurement of the MSC
ζ_A	The measurement over the maximum of A estimates of the MSC

8. REFERENCES

[1] L. H. Koopmans, *On the coefficient of coherence for weakly stationary stochastic processes*, Ann. Math. Statist., 35 (1964), pp. 532–549.

[2] N. R. Goodman, *Statistical analysis based on a certain multivariate complex Gaussian distribution (an introduction)*, Ann. Math. Statist., 34 (1963), pp. 152–177.

[3] M. Abramowitz and I. A. Stegun, ed., *Handbook of Mathematical Functions with Formulas, Graphs, and Mathematical Tables*, U. S. Government Printing Office, Washington, DC, 1964.

[4] W. Marsh, private communication.

[5] B. Epstein, *Elements of the theory of extreme values*, Technometrics, 2 (1960), pp. 27–41.

[6] G. C. Carter, *Receiver operating characteristics for a linearly thresholded coherence estimation detector*, IEEE Trans. Acoust., Speech, Signal Processing, ASSP-25 (1977), pp. 90–92.

[7] R. Trueblood and D. Alspach, *Multiple coherence as a detection statistic*, Naval Ocean Systems Center, Technical Report 265, July 1978.

[8] L. H. Koopmans, *On the multivariate analysis of weakly stationary stochastic processes*, Ann. Math. Statist., 35 (1964), pp. 1765–1781.

[9] R. A. Fisher, *The general sampling distribution of the multiple correlation coefficient*, Proc. Royal Soc., Series A, 121 (1928), pp. 654–673.


DAT
FILM